J. Fluid Mech. (2003), *vol.* 493, *pp.* 219–229.
DOI: 10.1017/S0022112003005536 Printed in the United Kingdom

A new family of uniform vortices related to vortex configurations before merging

By C. CERRETELLI AND C. H. K. WILLIAMSON

Sibley School of Mechanical and Aerospace Engineering, Upson Hall, Cornell University, Ithaca, NY 14853-7501, USA

(Received 21 March 2003 and in revised form 4 June 2003)

Stimulated by experimental observations of vortex merging, we compute a new family of uniform-vorticity steady solutions of the Euler equations in two dimensions. In experiments with two co-rotating vortices, one finds that, prior to the convective merging phase, and the formation of vortex filaments, the initial pair diffuses into a single structure (with two vorticity peaks) in the form of a symmetric 'dumb-bell'. In the present computations, our exploration of the existence of vortex solutions has been guided by the streamline patterns of the co-rotating reference frame, and by the simple concept that the vortex boundary must be one of these streamlines. By varying the parameters which define the vortex patches, we find a family of vorticity structures which pass from the limiting case of point vortices, through the case of two equal co-rotating uniform vortices (as previously computed by Saffman & Szeto 1980; Overman & Zabusky 1982; Dritschel 1985), to the regime where the vortices touch in the form of a dumb-bell. Further exploration of this family of solutions leads to an elliptic vortex, which joins precisely to the local transcritical bifurcation from elliptic vortices with $n=4$ perturbation symmetry that was found by Kamm (1987) and Saffman (1988). Finally, one reaches a limiting 'cat's-eye' vortex patch of two-fold symmetry ($m=2$), which constitutes an extension to the limiting shapes of m-fold symmetry ($m>2$) found by Wu, Overman & Zabusky (1984).

1. Introduction

A great deal of attention has been paid, in previous years, to the problem of the equilibrium solutions for a pair of equal uniform vortices as they rotate around one another in irrotational fluid. The boundaries of these shapes were first determined in 1980 by Saffman & Szeto, and also by Zabusky (1980), Landau (1981), and Dritschel (1985, 1995). A central result coming from these studies is that, if the vortex core radius is sufficiently large, then stable equilibrium solutions do not exist. (This occurs when $R/b>0.31$, at some point prior to the two vortices touching, where $R=\sqrt{A/2\pi}$ is the equivalent core size of the vortex, of area $A/2$ and b is the distance between the vortex centroids). Overman & Zabusky (1982) analysed the behaviour of perturbed initial configurations for $R/b>0.3125$, demonstrating that co-rotating vortices rapidly deform, generate filaments and ultimately merge into a single structure. Many studies have subsequently assumed that, once two separate vortices reach a certain size, this theoretical result might signal the onset of merging of real vortices. In the studies above, a family of equilibrium solutions was found, whose limiting case was given as two distinctly non-circular vortices, which almost touch. However, experimental results differ from this picture, and one actually finds that the two vortices diffuse

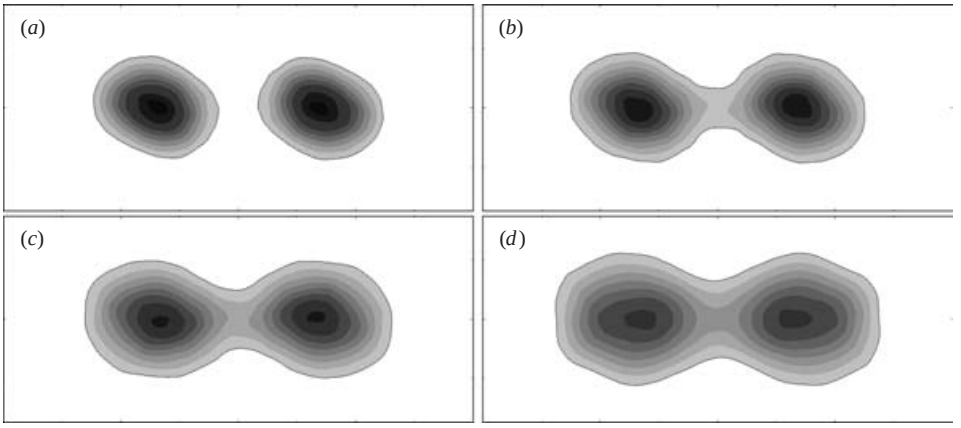

FIGURE 1. Vorticity fields during the merging process of two co-rotating vortices, as seen in a reference frame rotating with the vortex pair. These data are taken when the merging process is in the diffusive stage (prior to the generation of filaments and the convective merger stage, where vortices are pushed towards each other), and the two vortices undergo a diffusive growth while keeping their distance constant. (*a*) $t = 2.1$ s; (*b*) $t = 6.3$ s; (*c*) $t = 9.8$ s; (*d*) $t = 13.3$ s. Vorticity contours levels are in steps of $\Delta\omega = 0.05\,\mathrm{s}^{-1}$, with the lowest contour level being $\omega = 0.15\,\mathrm{s}^{-1}$. Vorticity is counter clockwise. $Re = \Gamma/\nu = 530$.

into a single symmetric rotating vortex (further described below), well before they start merging.

In recent experimental studies (Meunier & Leweke 2001; Cerretelli & Williamson 2003), it has been found that, prior to the generation of filaments and convective merger (the process where the vorticity peaks rapidly move towards each other), two equal co-rotating vortices undergo a diffusive growth, while they rotate around one another, keeping their separation distance constant. The typical evolution of the vorticity field for this diffusive stage is shown in figure 1, where we employ a reference frame rotating with the vortex pair. (An explanation of the use of the particle image velocimetry (PIV) technique to determine vorticity, and the experimental arrangement leading to these results, are found in Cerretelli & Williamson (2003). Of course, these shapes represent a minimum vorticity contour level, and it is clear that very weak vorticity will exist outside these shapes that makes a negligible contribution to the merger; see Cerretelli & Williamson (2003)). Rather than remain as two separate vortices, the vorticity diffuses into a single symmetric 'dumb-bell' shape (but which has two peaks of vorticity), and at some point thereafter the mutual vortex deformation leads to filamentation and vortex merging.

The principal vorticity dynamics can be usefully understood by employing a co-rotating reference frame. In figure 2, we show only the principal regions of the flow in such a reference frame, by extracting the separatrices of the co-rotating streamline pattern. Here we define an *inner core region*; an *inner recirculation region*, where fluid can travel around both vortices; and an *outer recirculation region*, where the fluid rotation is opposite to the rotation within the cores. Such streamlines were computed by Dritschel (1985) and by Melander, Zabusky & McWilliams (1988) for inviscid vortices. In this work, following the recent study of Cerretelli & Williamson (2003), we choose the nomenclature above, since we want to stress the distinction between the *inner region* and *the outer region*, because the separatrix between these areas is significant to the existence of equilibrium solutions.

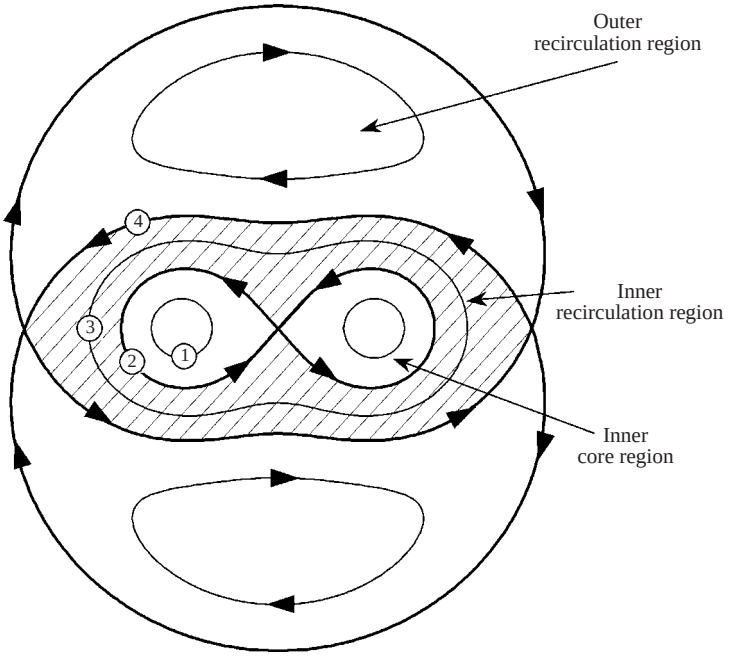

FIGURE 2. Diagram defining the regions of the flow field bounded by separatrices of the co-rotating stream function.

In this study, motivated by our experimental observations, we search for uniform-vorticity patches, using the simple physical concept that the boundaries of steady vortex patches must also be streamlines of the co-rotating reference frame. By observing the co-rotating set of streamlines in figure 2, one might suspect the existence of not only a pair of uniform vortices as found in previous works (as represented by streamline 1), but also the limiting case where the two vortices touch at a point (streamline 2), as well as possibly such shapes as represented by streamline 3, namely the dumb-bell shape. If such dumb-bells exist, as are found in experiment, then one would deduce that the limiting shape will be the one that forms the separatrix 4 between the inner and outer flow regions. One can readily see that any shape larger than the separatrix 4 will necessarily become deformed, producing filaments. We seek the existence of such uniform-vorticity topologies suggested above, and their precise shapes.

2. Equilibrium solutions to the Euler equations

In this paper, we obtain new equilibrium uniform-vorticity solutions to the Euler equation numerically. For a steady vortex configuration rotating with angular velocity Ω relative to the origin, the fluid velocity measured in a frame rotating at a rate Ω is tangent to the vortex boundaries (Dritschel 1985). Physically, in the rotating reference frame, it is straightforward to imagine that a vortex boundary of a steady vortex configuration must be a streamline of the flow field. This is equivalent to saying that the rotating-frame stream function must be constant on this boundary:

$$\psi(X, Y) - \tfrac{1}{2}\Omega(X^2 + Y^2) = C \tag{2.1}$$

where (X, Y) define points on the vortex boundary, and C is a constant. The stream function of the flow is given by

$$\psi(x, y) = \frac{\omega}{4\pi} \int \int_D \log[(x - x')^2 + (y - y')^2] \, dx' \, dy' = C \tag{2.2}$$

where ω is the uniform vorticity of the patch D. This equation is obtained by solving $\nabla^2 \psi = \omega$ in term of the Green function of the problem. The parameters C and Ω can be determined as follows:

$$\Omega = 2 \frac{\psi(X_A, Y_A) - \psi(X_B, Y_B)}{X_A^2 + Y_A^2 - X_B^2 - Y_B^2}, \quad C = \psi(X_A, Y_A) - \tfrac{1}{2} \Omega \left(X_A^2 + Y_A^2 \right) \tag{2.3}$$

where A and B are any two convenient locations on the vortex boundary. The numerical method used is essentially the iterative scheme employed by Pierrehumbert (1980) and Dritschel (1985) to which the reader should refer for details. Where we differ is in the choice of a new vortex shape, and rather than linearizing equation (2.1) about a good guess for the boundary shape (in order to determine the correction to this shape), we employ the streamlines of the flow in a co-rotating reference frame for advancing to successive steps in the iteration. A reasonable initial guess for the boundary shape of a uniform vortex could simply be made by choosing one of the streamlines close to (and outside) the boundary of a previous solution. We then compute the co-rotating stream function due to the new vortical flow field, using equations (2.1)–(2.3). The streamline which minimizes the area difference compared with the starting boundary shape is chosen as the boundary shape for the following iteration, and typically we found that after 6–8 iterations the solution converged such that the relative difference in the area between two successive solutions fell below 10^{-4}. The domain was uniformly discretized, with the grid spacing being one hundredth of the distance between the vortices.

By stepping from one steady shape to another, using the simple approach outlined above, our vortex patches are gradually enlarged, as shown in figure 3. The co-rotating vortex configurations (a and b) are in precise agreement with the shapes computed by Saffman & Szeto (1980) (the cases they list as $h = 1.5$ and $h = 0.95$). We subsequently also find the limiting case where the two vortices remain as separate entities, but they just touch at a single point, shown as the 'critical vortex pair' in (c) of figure 3. (The area of this shape is found to be $A/2b^2 = 0.3122$, which is in precise agreement with the computations of Kamm (1987) and Saffman (1988); see figure 9.6–1 in Saffman (1992)). The boundary of this critical vortex pair coincides with the separatrix (streamline 2 in figure 2) which separates the inner core region of the flow from the inner recirculation region. We stopped the computations at this point, under the apprehension that this was indeed the largest steady vortex which could be computed in this family. However, as we also plotted the co-rotating streamline pattern for each case we were able to observe that streamlines, even larger than the critical vortex pair, could perhaps deliver steady vortex configurations, more representative of the symmetric diffused vortices in experiment. We thus extended our study beyond the critical streamline 2, to include such streamlines as 3 (see figure 2). This exploration led us to define new steady shapes such as the dumb-bell, typified by the simply connected vortex patches in (d) and (e) of figure 3. As the exploration of these new shapes progressed, the thin region connecting the two lobes of the dumb-bell widened out, and the concave boundary of this region flattens out, ultimately giving the limiting shape of the dumb-bells as the 'sausage' shape (f). What is interesting also is that by continuing beyond the sausage, one arrives at a precise ellipse (shape g)

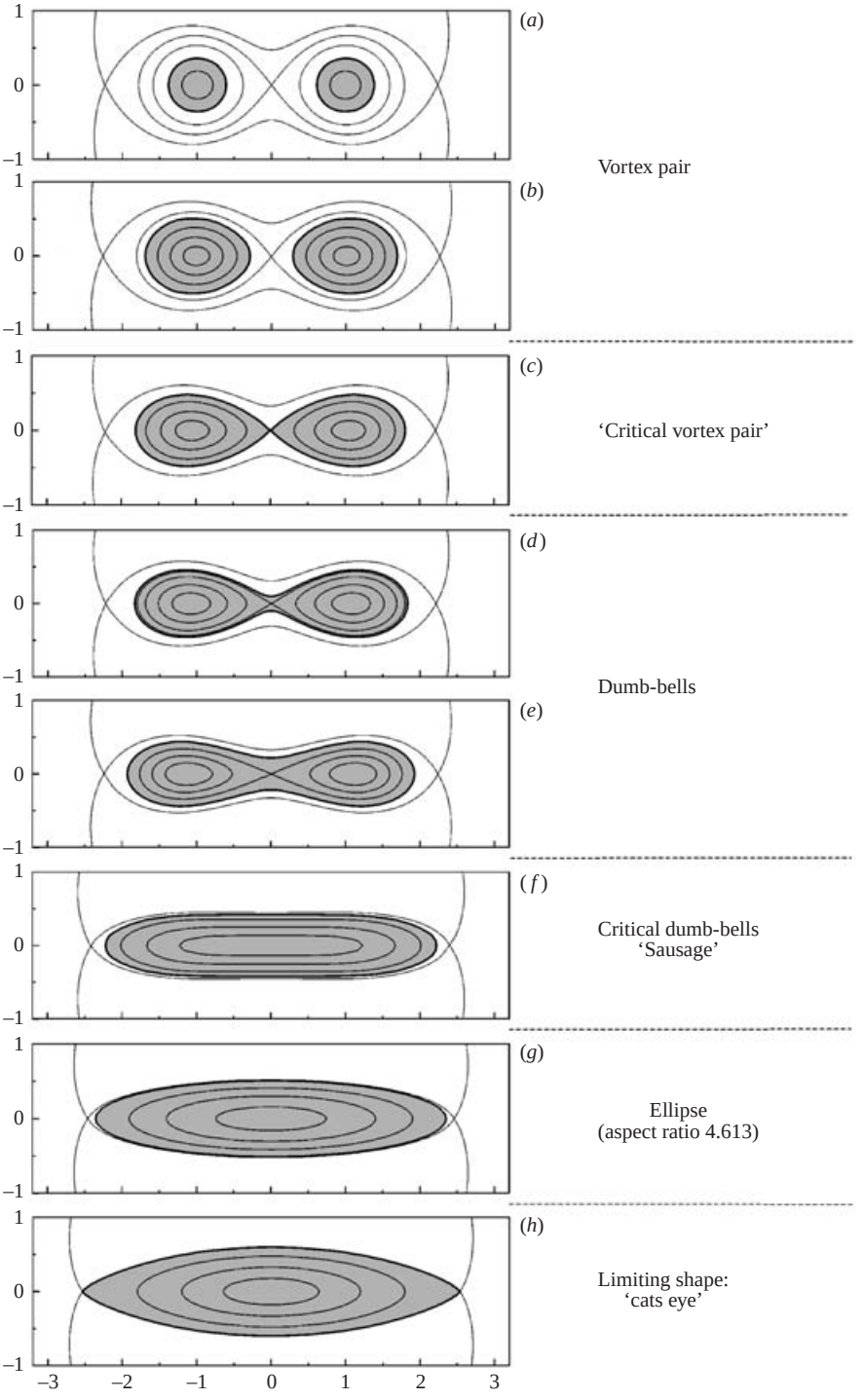

FIGURE 3. Shapes of the equilibrium solutions and co-rotating streamlines. The boundaries of the solutions are a streamline in a reference frame rotating with the vortices.

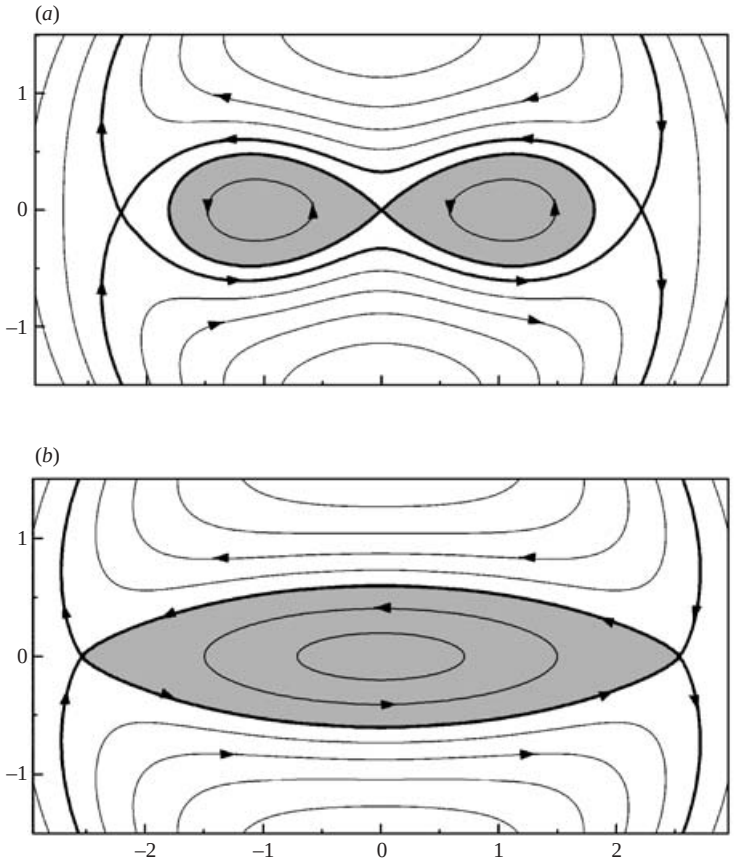

FIGURE 4. Limiting equilibrium solutions and co-rotating streamlines for (*a*) two touching co-rotating vortices (a critical vortex pair) and (*b*) a simply connected patch of vorticity (limiting cat's-eye vortex patch). Limiting shapes have 90° corners, and coincide with the separatrices of the co-rotating stream function. All separatrices are shown in bold lines.

of aspect ratio $L/h = 4.613$, which, although surprising initially, actually ties in well with a previous result of Kamm (1987) and Saffman (1988) (described below).

The limiting case for the whole family of solutions ultimately becomes a 'cat's-eye' shape, as shown by vortex (*h*). In an analogous manner to the limiting 'critical vortex pair', the boundary of this vortex coincides with the separatrix 4 of the streamline pattern (see figure 2) which separates the inner region from the outer recirculation region. These limiting vortex solutions, whose boundaries form the separatrices of their streamline patterns, are shown in greater detail in figure 4. Beyond the cat's-eye shape, any equilibrium solution, if it existed, would have to include uniform vorticity which extended all the way round the outer recirculation region. No equilibria were found beyond the cat's eye. The principal dimensions for these different shapes, making up this family of vortices, are included in table 1.

The coincidence of the boundary of the limiting vortex shape and the separatrix which separates the inner–outer flow regions appears to be a general property for other equilibrium solutions of *m*-polygonal symmetry. Vortices with such symmetries have been computed by Deem & Zabusky (1978), who discovered a whole set of what they call "V-states", or families of uniform vortices with *m*-polygonal symmetry,

		L/h	h_0/h	$2L/b$	R/b	$A/2b^2$	Ω/ω
(*a*)	Vortex pair	3.8603	–	1.3813	0.1870	0.1099	0.0359
(*b*)	Vortex pair	3.3506	–	1.6935	0.2969	0.2769	0.0912
(*c*)	Critical vortex pair	3.7555	0.0	1.8124	0.3152	0.3122	0.1078
(*d*)	Dumb-bell	4.0044	0.2173	1.8356	0.3114	0.3047	0.1097
(*e*)	Dumb-bell	4.3781	0.4975	1.9290	0.3233	0.3283	0.1154
(*f*)	Critical dumb-bell 'Sausage'	5.2711	1.0	2.2202	0.3611	0.4097	0.1368
(*g*)	Ellipse	4.6116	1.0	2.3556	0.3876	0.4720	0.1465
(*h*)	Limiting shape: 'cat's eye'	4.2431	1.0	2.5416	0.4157	0.5428	0.1556

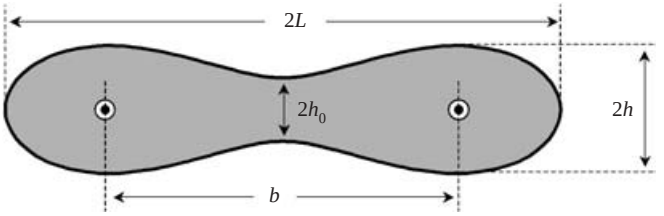

TABLE 1. Properties of the equilibrium solutions.

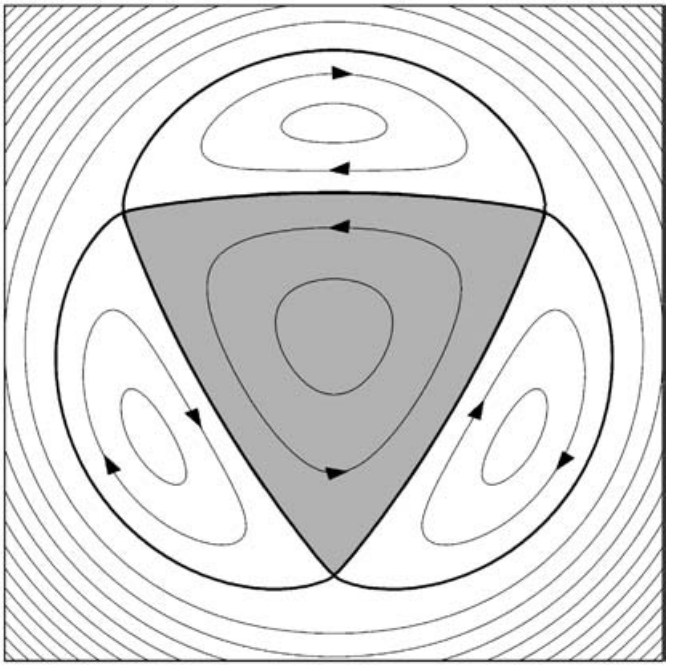

FIGURE 5. Limiting equilibrium solutions and co-rotating streamlines for a uniform patch (shaded region) with three-fold polygonal symmetry. This limiting shape (defined by the bold lines) has 90° corners, and coincides with the separatrix of the co-rotating stream function. Separatrices are shown as bold lines.

having three sides, four sides, etc. We have also computed the limiting (largest) shape, in the case of $m = 3$ (previously computed by Wu, Overman & Zabusky (1984), and by Overman (1986). We employed one of their equilibrium shapes as a starting point for our iterative scheme), and exhibit this result in figure 5. In our case, we have,

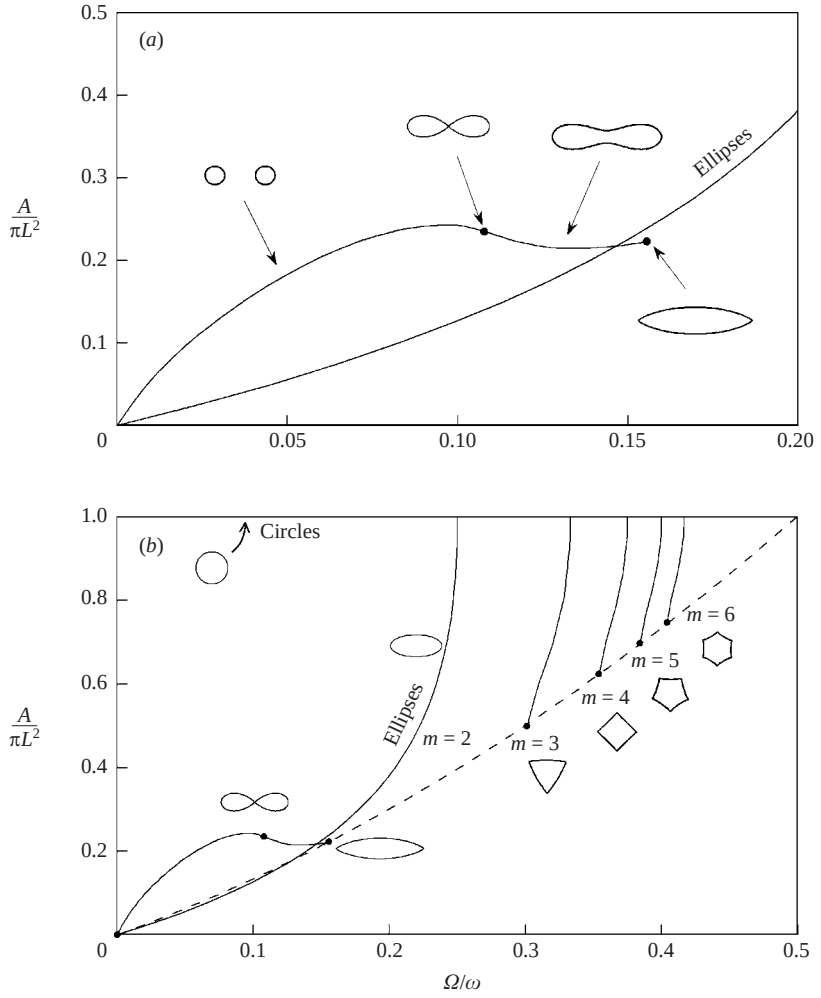

FIGURE 6. Solution paths for the co-rotating vortex pair and the single rotating vortex. In (*a*) the different parts of the path corresponding to either two distinct vortices or to a single patch are shown, together with the limiting cases. The point at which our solutions bifurcate from the Kirchhoff ellipses is also shown. In (*b*) the path of our computed solution is compared to all the previously computed paths for a single rotating vortex, as computed by Wu *et al.* (1984). There appears to be an envelope that embraces all the limiting shapes with *m*-polygonal symmetry.

as a part of our approach, also found the streamlines of the co-rotating reference frame, and one can see that the limiting shape boundary does indeed coincide with the separatrix streamline, bounding an inner flow region from an outer one. Such boundaries also have 90° corners, which is consistent with the studies of Saffman & Szeto (1981) and Pullin (1992), and also follows the study of Overman (1986), who proved that such vortex patches can only have corners with angles of of either 90° or 0° (the latter being cusps).

The manner in which this family of uniform-vortex solutions corresponds with previous studies of equilibrium solutions is of interest. For this discussion, we shall refer to the plane of the vortex area ($A/\pi L^2$) versus rotational velocity of the vortex shape (Ω/ω), in figure 6. The present family of vortex shapes in figure 6(*a*) starts at

the origin, representing a pair of point vortices, passes through the regime of vortex pair configurations, to the critical vortex pair where the two vortices touch at a point (shown with a symbol), then passes across the curve that represents ellipses, and finally reaches the point in the plane corresponding to the limiting cat's-eye shape. If we look at figure 6(*b*), we can see that the horizontal upper boundary of the plot represents Rankine (circular) vortices of uniform vorticity, for which $A/\pi L^2 = 1$. The curve for the Kirchhoff elliptic vortices starts at this upper boundary, and gradually, as the aspect ratio of the vortex increases, this curve approaches the origin, in which case the Kirchhoff ellipse becomes a vortex sheet of length $2L$, as noted by Batchelor (1967).

The location at which our family curve passes across the ellipse family curve is particularly interesting. The stability analysis of Moore & Saffman (1971) shows that one expects an infinite number of bifurcations, for disturbances which have n-fold symmetry relative to the elliptic vortex, each bifurcation occurring for a particular value of aspect ratio (L/h). In fact, Kamm (1987) went on to find the first three of these bifurcations in the vicinity of the ellipse solutions; namely for aspect ratio $L/h = 3.0$ (which confirms a classic result of Love 1893), for aspect ratio $L/h = 4.611$ and for $L/h = 6.197$. These bifurcations correspond to disturbances with $n = 3, 4, 5$. Our curve of solutions, in the plane of $A/\pi L^2$ versus Ω/ω, in figure 6, passes across the ellipse curve at precisely the $n = 4$ bifurcation found by Kamm (1987) and Saffman (1988), at which point we compute the aspect ratio to be $L/h = 4.613$. This is consistent with the fact that this bifurcation is transcritical, thus admitting such a solution curve that cuts across the ellipse curve in the manner here, whereas the $n = 3$ and 5 cases are subcritical pitchfork bifurcations. It is also consistent with the fact that, either side of the ellipse curve, our family of shapes evidently conforms to a 4-fold perturbation to an ellipse.

The limiting case of our family of shapes appears to be in the same class of vortices as the limiting shapes (also included in figure 6) computed by Wu *et al.* (1984) for the $m = 3, 4, 5$ and 6-fold symmetric 'V-states' previously found in Deem & Zabusky (1978) (limiting shapes which have three sides, four sides, etc.). The $m = 3$–6 branches, as shown in figure 6, arise out of bifurcations from the Rankine vortex, although our family of solutions arises in quite a different manner. However, all of these shapes, including our cat's-eye vortex have polygonal symmetry with 90° corners. One can deduce a best-fit curve through the $m = 3$–6 data in figure 6 (including the origin, and also the point ($A/\pi L^2 = 1$; $\Omega/\omega = 0.5$), which represents a perturbation to the Rankine vortex when $m \to \infty$):

$$\frac{A}{\pi L^2} = 1.173\frac{\Omega}{\omega} + 1.662\left(\frac{\Omega}{\omega}\right)^2. \tag{2.4}$$

The curve passes precisely through our limiting cat's-eye shape, which further suggests that our limiting vortex is the $m = 2$ case corresponding to the limiting solutions $m = 3$–6 found by Wu *et al.* (1984).

3. Concluding remarks

In summary, we have discovered a new family of equilibrium uniform-vorticity configurations, guided by the simple approach that the boundaries of these shapes must be streamlines in the co-rotating reference frame. The key to finding these shapes has been, for each vortex patch, to plot a set of flow streamlines, which naturally then suggests the choice of a further equilibrium vortex shape, thereby enlarging the

family of solutions. Our exploration of these vortices has therefore been firmly based on the physical flow dynamics.

Our family of vortex shapes starts with the vortex pair configurations which are agreement with previous studies (Saffman & Szeto 1980; Overman & Zabusky 1982; Dritschel 1985). We have found that the limiting case of the two vortex problem is where they touch at a point, in a critical vortex pair configuration. However, triggered by experimental observations, where the physical vortices actually diffuse into a dumb-bell vortex before the two vortices are pushed together in the convective merging stage, we have discovered from our computations that such uniform-vorticity dumb-bell configurations exist, whose shapes are similar to those found experimentally. Of course, in the real situation, the vorticity is distributed non-uniformly and filaments are always visible, if one considers sufficiently small levels of vorticity (Le Dizes & Verga 2002). However, the succession of vortices passing from vortex pairs to dumb-bells approximately represents the temporal change of vortex shape as the real vortices diffuse before convective merger.

For shapes larger than the dumb-bells, the family of vortex solutions includes an ellipse, which is precisely the elliptic vortex shape for which Kamm (1987) and Saffman (1988) found a transcritical bifurcation of $n = 4$ perturbation symmetry for the set of ellipses. Further along the family of vortices, by varying our parameters, we reach a limiting shape, beyond which there is no further solution, and this takes on the form of a cat's eye. This appears to be the $m = 2$ case, corresponding with the $m > 2$ limiting shapes found by Wu *et al.* (1984), all of which have corners of 90°, and which represent the ends of the families of m-fold polygonal 'V-states' found by Deem & Zabusky (1978).

It would be interesting to study the stability of our vortex shapes including the dumb-bell shapes. However, the stability analysis, for the vortex pair configurations, has been conducted by Dritschel (1985), and also by Saffman & Szeto (1980), who used an energy argument. Dritschel deduced that vortex pairs whose area exceeds a certain value ($A/2b^2 > 0.3096$), were unstable. This type of result, and the inviscid simulations of Overman & Zabusky (1982), and others, suggest that one might expect vortices to start to convectively merge and come together at this point. However, one might note that in experiments, the vortices are distributed (with well-defined vorticity peaks) rather than uniform patches. We observe the vortices to evolve all the way to symmetric dumb-bell shapes before they start the deformation process, the generation of filaments, and the corresponding convective merger, where the vortices are pushed together by the action of the antisymmetric vorticity (Cerretelli & Williamson 2003).

As a final point, it is intriguing to note that Kamm (1987), using an energy argument, found that some shapes, comprising those from the ellipse bifurcation towards the 'sausage' critical dumb-bell shape, are stable. Therefore it is possible that a range (or all) of the dumb-bell shapes are stable, despite the fact that the largest of the vortex pair configurations appear to become unstable ($A/2b^2 > 0.3121$), using similar energy considerations. A stability analysis for the whole family of vortex shapes in this paper would be enlightening.

The support from the Ocean Engineering Division of O.N.R., monitored by Dr Tom Swean, is gratefully acknowledged (O.N.R. Contract Numbers N00014-94-1-1197 and N00014-95-1-0332). The work of C. Cerretelli was also supported by the Rotary Foundation (Rotary International Ambassadorial Scholarship, 1998/99) and by the Gruppo Dirigenti FIAT (Borsa di Studio "Carlo Ghiglieno", 1999/2000). We acknowledge with thanks the insightful comments of the reviewers and editor of this

paper. We have benefited greatly from many discussions with Dr D. I. Pullin, Dr S. Leibovich, Ing. G. Nikitina and Dr C. Champagne.

REFERENCES

Batchelor, G. K. 1967 *An Introduction to Fluid Dynamics*. Cambridge University Press.

Cerretelli, C. & Williamson, C. H. K. 2003 The physical mechanism for vortex merging. *J. Fluid Mech.* **475**, 41–77.

Deem, G. S. & Zabusky, N. J. 1978 Vortex waves: stationary "V states", interactions, recurrence, and breaking. *Phys. Rev. Lett.* **40**, 859–862.

Dritschel, D. G. 1985 The stability and energetics of corotating uniform vortices. *J. Fluid Mech.* **157**, 95–134.

Dritschel, D. G. 1995 A general theory for two-dimensional vortex interactions. *J. Fluid Mech.* **293**, 269–303.

Kamm, J. R. 1987 Shape and stability of two-dimensional vortex regions. PhD thesis, Caltech, Pasadena, USA.

Landau, M. 1981 The structure and stability of finite area vortex regions of the two-dimensional Euler equations. PhD thesis, University of Pittsburgh, USA.

Le Dizes, S. & Verga, A. 2002 Viscous interactions of two co-rotating vortices before merging. *J. Fluid Mech.* **467**, 389–410.

Love, A. E. H. 1893 On the stability of certain vortex motions. *Proc. Lond. Math. Soc.* **25**, 18–42.

Melander, M. V., Zabusky, N. J. & McWilliams, J. C. 1988 Symmetric vortex merger in two dimensions: causes and conditions. *J. Fluid Mech.* **195**, 305–340.

Meunier, P. & Leweke, T. 2001 Three-dimensional instability during vortex merging. *Phys. Fluids* **13**, 2747–2750.

Moore, D. W. & Saffman, P. G. 1971 Structure of a line vortex in an imposed strain. In *Aircraft Wake Turbulence* (ed. D. E. Olsen, A. Goldburg & M. M. Rogers), pp. 339–354. Plenum.

Overman, E. A. 1986 Steady state solutions of the Euler equations in two dimension II. Local analysis of limiting V-States. *SIAM J. Appl. Maths* **46**, 765–800.

Overman, E. A. & Zabusky, N. J. 1982 A merging criterion for two-dimensional co-rotating vortices. *Phys. Fluids* **25**, 1297–1305.

Pierrehumbert, R. T. 1980 A family of steady, translating vortex pairs with distributed vorticity. *J. Fluid Mech.* **99**, 129–144.

Pullin, D. I. 1992 Contour dynamics methods. *Annu. Rev. Fluid Mech.* **24**, 89–115.

Saffman, P. G. 1988 The stability of vortex arrays to two and three dimensional disturbances. *Fluid Dyn. Res.* **3**, 13–21.

Saffman, P. G. 1992 *Vortex Dynamics*. Cambridge University Press.

Saffman, P. G. & Szeto, R. 1980 Equilibrium shapes of a pair of equal uniform vortices. *Phys. Fluids* **23**, 2339–2342.

Saffman, P. G. & Szeto, R. 1981 Structure of a linear array of uniform vortices. *Stud. Appl. Maths* **65**, 223–2248.

Wu, H. M., Overman, E. A. & Zabusky, N. J. 1984 Steady-state solutions of the Euler Equations in two dimensions: rotating and translating V-States with limiting cases. I. Numerical algorithms and results. *J. Comput. Phys.* **53**, 42–71.

Zabusky, N. J. 1980 Contour dynamics: a boundary-integral evolutionary method for incompressible dissipationless flows. In *Numerical Methods for Engineering: 2nd Intl Congress* (ed. E. Absi). Dunoud.